

## Viscosity of Liquid Di-isodecyl Phthalate at Temperatures Between (274 and 373) K and at Pressures up to 140 MPa

Fotos Peleties and J. P. Martin Trusler\*

Department of Chemical Engineering, Imperial College London, South Kensington Campus, London SW7 2AZ, United Kingdom

**ABSTRACT:** We report measurements of the viscosity of liquid di-isodecyl phthalate (DIDP) and a correlation determined therefrom. The viscosity of DIDP was measured at temperatures between (298.15 and 373.15) K and pressures between (0.1 and 140) MPa with a relative uncertainty of 2 % by means of a new vibrating-wire viscometer. Additional measurements were made at a constant pressure of 0.1 MPa in the temperature range (274.07 to 368.21) K by means of capillary viscometers, with a relative uncertainty of 1 %. The results have been represented by a correlating equation containing six adjustable parameters with an average absolute relative deviation of 0.9 % and a maximum absolute relative deviation of 2.9 %. The available literature data are found to be generally in good agreement with our correlation at temperatures between (293 and 373) K at pressures up to 140 MPa, even when the corresponding viscosity is up to a factor of 10 greater than the largest viscosity measured in this work. A two-parameter correlation for the viscosity of DIDP at  $p = 0.1$  MPa is also presented that represents the present results and selected data from the literature with an absolute relative deviation of 0.5 % and a maximum absolute relative deviation of 1.7 % at temperatures of (273 to 369) K. Viscosities of 1-methylnaphthalene at  $T = 298.15$  K and pressures up to 140 MPa were also measured for purposes of verification.

### INTRODUCTION

Di-isodecyl phthalate (DIDP) has been proposed as an industrial standard reference liquid for the calibration of viscometers operating in the viscosity range (50 to 125) mPa·s at temperatures near 298.15 K.<sup>1–4</sup> A review of the available data for the viscosity of DIDP at  $p = 0.1$  MPa and at temperatures between (288.15 and 308.15) K has recently been published, together with recommended reference values at  $T = (293.15, 298.15, \text{ and } 303.15)$  K.<sup>5</sup> A number of commercially available reference liquids, with certified values of viscosity at specified temperatures, are available for the calibration of viscometers at ambient pressure. No such fluids exist for use at high pressures, and this makes the calibration and/or validation of secondary viscometers at  $p > 0.1$  MPa problematic. However, DIDP may be useful as an industrial reference fluid for the calibration of viscometers in extended ranges of temperature and pressures, and the present work was undertaken with that objective in mind. In the case of DIDP, there is a lack of experimental viscosity data at high pressures obtained with primary instruments that do not themselves require calibration at high pressures. The present work addresses that gap.

### MATERIALS

Analysis grade DIDP (CAS number 26761-40-0, mole fraction purity  $x > 0.998$ ) was purchased from Merck, and 1-methylnaphthalene (CAS number 90-12-0,  $x > 0.98$ ) was purchased from Fluka. Viscosity standard liquids N2, N10, N35, and N100 were purchased from Cannon. Before use, the DIDP was dried over grade 4A molecular sieves and degassed under vacuum. The water content was not measured. As discussed in the literature,<sup>5</sup> commercially available DIDP is a mixture of isomers having the generic structure depicted in Figure 1 with varying degrees of branching in the C<sub>10</sub>H<sub>21</sub> chains. 1-Methylnaphthalene was

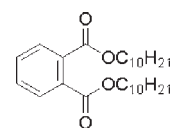


Figure 1. Structure of di-isodecyl phthalate (DIDP).

degassed by refluxing at ambient pressure. Other chemicals were used as received.

### APPARATUS

The measurements under elevated pressure were made using a new vibrating-wire viscometer.<sup>6</sup> The sensor, illustrated in Figure 2, comprised a centerless-ground tungsten wire of free length 52 mm and diameter 0.3 mm (Metal Cutting Corp., New Jersey, USA) stretched between a pair of clamps, fabricated from Monel K500, fitted to either end of a tube of inner diameter (i.d.) 9.9 mm and wall thickness 2.5 mm fabricated from Shapal-M machinable ceramic. This ceramic has a linear thermal expansion coefficient of  $4.4 \cdot 10^{-6} \text{ K}^{-1}$  which,<sup>7</sup> being very close to that of tungsten, ensured that the wire tension remained approximately constant when the temperature was varied. To facilitate location of the sensor within the pressure vessel, the outer diameter (o.d.) of the ceramic tube was enlarged to 17.9 mm over a 3 mm long section in the middle to form a lip. The ends of the tube were also machined to fit sockets in the clamps, and the joints were bonded with an epoxy resin (Stycast 2850 FT with catalyst 9). For assembly, with the sensor orientated vertically, a length of tungsten wire was passed through, secured to the top clamp, and tensioned by attaching a mass of approximately 1.6 kg to its

Received: November 22, 2010

Accepted: February 5, 2011

Published: February 28, 2011

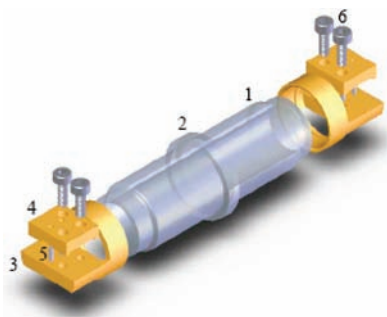


**Figure 2.** Exploded view of the vibrating-wire sensor: (1) flow tube; (2) retaining lip; (3) end support; (4) clamping plate; (5) alignment pin; (6) M2 screws.

lower end. Pins located in the end pieces were used to align the tungsten wire along the axis of the sensor. The wire was left in this condition for a period of typically 24 h before the lower end-clamp was tightened and, finally, the excess wire protruding from each end cut off. Tensioned in this way, the fundamental transverse resonance frequency of the wire in ambient air was approximately 1200 Hz.

The pressure vessel was a custom-made high-pressure nipple of o.d. 30 mm fabricated from AISI type 660 stainless steel. The nipple was bored through to an i.d. of 15.0 mm and then counter-bored to 18.0 mm from each end, leaving a small shoulder of the smaller i.d. in the center of the vessel. The ends of the nipple were coned at an angle of 59°, threaded externally (left-hand M30), and fitted with retaining nuts and screw collars. Custom-made reducing unions, fabricated from cold-drawn AISI type 316 L stainless steel, were used to connect either end of the vessel to standard 6.35 mm o.d. coned-and-threaded high-pressure tubing. One end of the nipple was also threaded on the inner bore (M20 × 22 mm) to accept a threaded stainless-steel sleeve that fitted over one end of the sensor and, when screwed home, retained it by pressing the lip of the sensor against the shoulder inside the vessel. Stainless-steel and poly(ether ether ketone) (PEEK) washers were used either side of the lip on the sensor. This arrangement provided a rigid mounting of the sensor with minimal trapped volumes and provision, though the PEEK washer, to absorb differential thermal expansion.

The end clamps on the sensor were provided with screw terminals for the attachment of the electrical lead wires. A slot machined along the length of the ceramic tube permitted a 0.35 mm diameter polyimide-insulated copper wire to pass back from one end to the other so that the external lead wires could approach from one end only. Thereafter, four wires (two connected to each end of the sensor) passed along the inside of the pressure vessel and through a length of the connecting tubing to an hermetically sealed four-pin high-pressure connector (Green Tweed type 5672 4-pin connector) which was sealed to a custom-made union tee by means of Viton O-rings.

The sensor, located within the pressure vessel, was mounted between the poles of a permanent magnet assembly comprising a pair of 50.8 mm × 50.8 mm × 50.8 mm NdFeB magnet blocks yoked together by a mild steel “C” piece. This assembly provided a magnetic field of approximately 0.38 T at the midpoint between the poles at  $T = 298.15$  K. Tuning of the sensor to a pure mode was accomplished by rotation of the pressure vessel prior to tightening the connecting-tube unions.

A high-pressure syringe pump (Quizix model C-5000-20K-HC-AT) was used to deliver liquid to one end of the pressure vessel, while the other end was connected to a pressure transducer (Paroscientific model 420KR-HHT-101-CE, 138 MPa full scale) and a drain valve. The pressure vessel and pressure transducer were mounted within an environmental test chamber (Tenney model ETCU-09S2.SCY) which provided temperature control; this chamber was cubic in shape with a volume of approximately 0.25 m<sup>3</sup>. The temperature of the sensor was inferred from the readings of two platinum resistance thermometers (PRTs) that had been calibrated both at the temperature of the triple point of water and against a standard PRT over the full temperature range of the measurements. These PRTs were located in pockets machined in the reducing unions at either end of the tubular pressure vessel. Temperature stability and uniformity were within ± 0.02 K over the period of time required to make a measurement at a single temperature and pressure. The long-term stability was less good with variation of ± 0.15 K observed over a period of three days. The estimated expanded uncertainty of the temperature was 0.05 K, while the estimated expanded uncertainty of pressure was 0.03 MPa, both with coverage factors  $k = 2$ .

All measurements with the vibrating-wire sensor were made in steady-state forced mode, utilizing the fundamental transverse mode of oscillation. A lock-in amplifier with built-in sinusoidal signal generator was used to excite and detect the wire motion. The complex voltage  $V$  measured across the wire was assumed to conform to the following working equation:

$$V = \frac{\Lambda if}{f_0^2 - f^2(1 + \beta) + if^2(\beta' + 2\Delta_0)} + a + bi + cif \quad (1)$$

Here,  $\Lambda$  is an amplitude,  $f$  is the drive frequency, and  $f_0$  and  $\Delta_0$  are the resonance frequency and logarithmic decrement of the wire in vacuum. The quantities  $\beta$  and  $\beta'$  account for the added mass and damping arising from the fluid around the wire and are given by<sup>8,9</sup>

$$(\beta' + i\beta) = \frac{\rho}{\rho_s} \left[ i + \frac{4iK_1(\sqrt{i\Omega})}{\sqrt{i\Omega}K_0(\sqrt{i\Omega})} \right] \quad (2)$$

where

$$\Omega = 2\pi f \rho R^2 / \eta \quad (3)$$

Here,  $\rho$  and  $\eta$  are the density and viscosity of the fluid,  $\rho_s$  and  $R$  are the density and radius of the wire, and  $K_n$  is the modified Bessel functions of the second kind with order  $n$ .

The radius of the wire at  $T = 298.15$  K was measured by the supplier to be 300.3 μm with an expanded uncertainty of 1.2 μm. In the present work, the fluid density was an input parameter determined at each state point from an equation of state, and the logarithmic decrement under vacuum was inferred from a calibration measurement in ambient air. The viscosity of the liquid under study was then determined by means of a nonlinear optimization in which the values of  $\Lambda$ ,  $f_0$ ,  $\eta$ ,  $a$ ,  $b$  and  $c$  were adjusted to minimize the deviations between the experimental resonance data,  $V(f)$ , and eq 1.

The vibrating-wire viscometer was used as an absolute instrument: that is, the radius was taken to be that certified by the supplier. The 0.4 % relative uncertainty of that value propagates into a relative uncertainty in the viscosity of 0.8 %. Considering also the reproducibility of the instrument and the uncertainties in

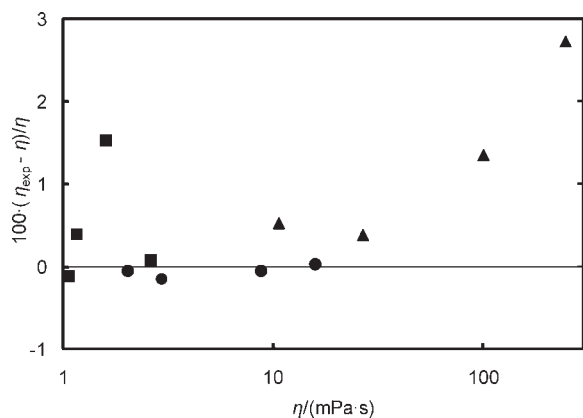


**Figure 3.** Deviations of the measured viscosity  $\eta_{\text{exp}}$  of standard liquids from the values  $\eta$  given by the manufacturer: ●, N10; ■, N35; ▲, N100.

temperature and pressure, we estimate an overall relative uncertainty of 2 % in the measured viscosity.

Measurements of the viscosity at ambient pressure were carried out with a set of four glass U-tube capillary viscometers (Poulten Selfe and Lee Ltd., UK), denoted A to D, covering the following ranges: A, (2 to 10)  $\text{mm}^2 \cdot \text{s}^{-1}$ ; B, (10 to 50)  $\text{mm}^2 \cdot \text{s}^{-1}$ ; C, (60 to 300)  $\text{mm}^2 \cdot \text{s}^{-1}$ ; and D, (200 to 1000)  $\text{mm}^2 \cdot \text{s}^{-1}$ . The viscometers were thermostatted in a glass water bath controlled with a stability and uniformity of  $\pm 0.02$  K. A cooling coil was fitted to the bath through which refrigerated fluid could be circulated for operation at temperatures below ambient. The temperature of the bath was measured with a calibrated PRT probe with an uncertainty of 0.05 K ( $k = 2$ ). The kinematic viscosity  $\nu$  was determined from the measured flow time  $t$  by means of the relation:

$$\nu = CT \quad (4)$$

where  $C$  is a constant determined by calibration. Viscometers A, B, and D were calibrated at  $T = 298.15$  K with Cannon standard liquids N2, N10, and N100, respectively, while viscometer C was calibrated by the supplier. The relative uncertainty of the flow time was always less than 0.2 %, and the estimated overall expanded uncertainty, including time, temperature, and calibration uncertainties, is 1.0 % ( $k = 2$ ).

## EXPERIMENTAL SECTION

To validate the apparatus, measurements were made on three viscosity-standard liquids (Cannon N10, N35, and N100) at ambient pressure and temperatures in the range (298.15 to 373.15) K and in 1-methylnaphthalene at  $T = 298.15$  K at pressures up to 120 MPa.

In the case of the three viscosity standard liquids, the manufacturer provided tabulated values of the viscosity and density over the full temperature range of the measurements and, for purposes of interpolation, these data were represented by polynomial function of temperature. The deviations of the experimental measurements from the interpolated manufacturer's data are shown in Figure 3 as a function of viscosity. Up to  $\eta = 100$   $\text{mPa} \cdot \text{s}$ , the absolute relative deviations do not exceed 1.5 %. The remaining point (N100 at  $T = 298.15$  K), corresponding to the highest viscosity studied, has a relative deviation of +2.7 %.

In the case of 1-methylnaphthalene, the density  $\rho$  at each state point was computed from the correlation reported by Caudwell

**Table 1.** Viscosity  $\eta$  (This Work) and Density<sup>10</sup>  $\rho$  of 1-Methylnaphthalene at  $T = 298.15$  K and Pressures  $p$

$p$	$\rho$	$\eta$	$p$	$\rho$	$\eta$
MPa	$\text{kg} \cdot \text{m}^{-3}$	$\text{mPa} \cdot \text{s}$	MPa	$\text{kg} \cdot \text{m}^{-3}$	$\text{mPa} \cdot \text{s}$
0.2	1019.7	2.90	80.0	1055.4	6.68
0.2	1019.6	2.89	120.1	1069.8	10.12
1.0	1020.1	2.93	120.1	1069.8	10.17
1.0	1020.1	2.92	79.9	1055.4	6.67
10.0	1024.8	3.24	79.9	1055.4	6.65
10.0	1024.8	3.24	39.9	1038.9	4.41
40.0	1039.0	4.42	39.9	1038.9	4.40
40.0	1039.0	4.42	1.0	1020.1	2.94
80.0	1055.4	6.65	1.0	1020.2	2.93

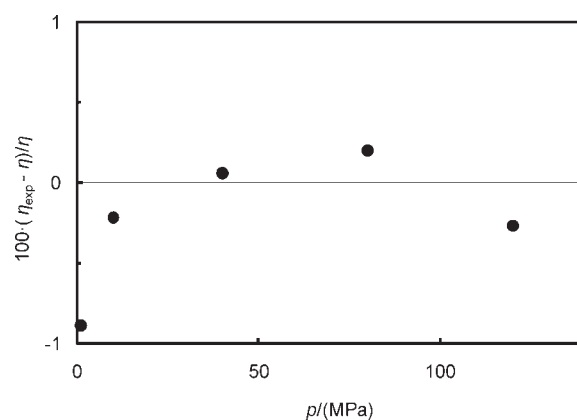


**Figure 4.** Deviations of the measured viscosity  $\eta_{\text{exp}}$  of 1-methylnaphthalene from the correlation of Caudwell et al.: ●,  $T = 298.15$  K.

et al.,<sup>10</sup> which has a stated relative uncertainty of 0.2 %. The experimental viscosities (together with the calculated densities) are reported in Table 1 and compared in Figure 4 with the viscosity correlation reported by Caudwell et al.,<sup>10,11</sup> which has a stated relative uncertainty of 2 %; the relative deviations lie between  $-1.2$  % and 0.2 %.

The vibrating-wire measurements on DIDP were conducted principally along four isotherms in the range (298.15 to 373.15) K with pressures up to the lower of 140 MPa and the pressure at which the viscosity reached approximately 230  $\text{mPa} \cdot \text{s}$ . A few measurements were also made at  $T = (305.15 \text{ and } 368.15)$  K at low pressures. The density of DIDP was computed from the equation of state recently reported by Peleties et al.,<sup>12</sup> which has a stated uncertainty of just 0.025 % and was derived from measurements of density, isobaric specific heat capacity, and speed of sound made on DIDP from the same lot as used in the present study. The experimental viscosities and the corresponding computed densities are given in Table 2.

Measurements of the kinematic viscosity of DIDP at  $p = 0.1$  MPa were performed at temperatures of (274.07 to 368.21) K and combined with densities from Peleties et al.<sup>12</sup> to obtain the shear viscosity  $\eta$ ; the results are given in Table 3.

## ANALYSIS

A reasonably accurate empirical representation of the  $\eta(T, p)$  surface is afforded by the modified Vogel–Fulcher–Tammann

Table 2. Viscosity  $\eta$  (This Work) and Density<sup>12</sup>  $\rho$  of DIDP at Temperatures  $T$  and Pressures  $p$ 

$p$	$\rho$	$\eta$	$p$	$\rho$	$\eta$	$p$	$\rho$	$\eta$
MPa	$\text{kg}\cdot\text{m}^{-3}$	$\text{mPa}\cdot\text{s}$	MPa	$\text{kg}\cdot\text{m}^{-3}$	$\text{mPa}\cdot\text{s}$	MPa	$\text{kg}\cdot\text{m}^{-3}$	$\text{mPa}\cdot\text{s}$
T = 298.15 K			T = 313.15 K			T = 343.15 K		
0.2	962.99	87.57	10.1	958.37	46.34	80.1	976.08	41.24
0.2	962.99	87.58	10.1	958.37	46.33	80.1	976.08	41.24
0.2	962.99	87.62	10.1	958.37	46.23	137.1	999.30	95.56
0.2	962.99	87.63	20.0	964.07	57.28	137.1	999.30	95.61
0.2	962.99	87.63	20.0	964.07	57.35	137.1	999.30	95.61
0.2	962.99	87.64	20.0	964.07	57.32	0.2	931.01	10.99
0.2	962.99	87.71	40.0	974.62	87.15	0.2	931.01	10.97
10.0	968.64	112.08	40.0	974.62	87.13	0.2	931.01	10.96
10.0	968.64	112.08	40.0	974.62	87.03	T = 368.15 K		
10.0	968.64	112.26	59.9	984.10	130.49	0.3	913.42	5.650
20.0	974.06	143.41	59.9	984.10	130.29	0.3	913.42	5.650
20.0	974.06	143.42	60.0	984.15	130.33	0.3	913.42	5.650
20.0	974.06	143.67	80.0	992.87	194.08	0.3	913.42	5.650
40.0	984.06	230.93	80.0	992.87	194.41	T = 373.15 K		
40.0	984.06	231.01	80.0	992.87	195.20	0.3	909.89	5.040
40.0	984.06	231.09	0.2	952.29	37.08	0.3	909.89	5.050
40.0	984.06	231.39	0.2	952.29	37.06	0.3	909.89	5.050
40.0	984.06	231.55	0.2	952.29	37.10	20.1	924.96	6.876
40.0	984.06	231.61	T = 343.15 K			20.1	924.96	6.876
0.2	962.99	87.61	0.2	931.01	11.20	20.1	924.96	6.866
0.2	962.99	87.66	0.2	931.01	11.19	40.0	937.92	9.055
0.2	962.99	87.71	0.2	931.01	11.20	40.0	937.92	9.075
T = 305.15 K			10.1	937.92	13.33	40.0	937.92	9.085
0.2	957.99	57.04	10.1	937.92	13.33	80.1	959.73	15.22
0.2	957.99	57.10	10.1	937.92	13.35	80.1	959.73	15.23
0.2	957.99	57.12	20.1	944.40	15.85	80.1	959.73	15.23
0.2	957.99	57.13	20.1	944.40	15.86	137.2	984.66	30.11
0.2	957.99	57.18	20.1	944.40	15.86	137.2	984.66	30.12
T = 313.15 K			40.0	956.07	22.04	137.2	984.66	30.15
0.2	952.29	37.38	40.0	956.07	22.05	0.3	909.89	4.920
0.2	952.29	37.38	40.0	956.07	22.05	0.3	909.89	4.920
0.2	952.29	37.32	80.1	976.08	41.22	0.3	909.89	4.920

Table 3. Viscosity  $\eta$  (This Work) and Density<sup>12</sup>  $\rho$  of DIDP at Temperatures  $T$  and Pressure  $p = 0.1$  MPa

$T$	$\rho$	$\eta$	$T$	$\rho$	$\eta$
K	$\text{kg}\cdot\text{m}^{-3}$	$\text{mPa}\cdot\text{s}$	K	$\text{kg}\cdot\text{m}^{-3}$	$\text{mPa}\cdot\text{s}$
274.07	980.19	606.7	327.83	941.80	19.32
274.35	979.99	588.6	343.53	930.67	11.15
283.03	973.75	265.9	343.33	930.81	11.09
282.95	973.81	270.2	343.24	930.87	11.10
298.25	962.86	87.67	368.54	912.98	5.577
305.26	957.85	57.43	368.21	913.21	5.627
313.27	952.15	37.41			

(VFT) equation:

$$\ln[\eta/(\text{mPa}\cdot\text{s})] = a + b(p/\text{MPa}) + \frac{c + d(p/\text{MPa}) + e(p/\text{MPa})^2}{(T - T_0)/\text{K}} \quad (5)$$

Table 4. Parameters in Equation 5

$a$	$b$	$c$	$d$	$e$	$T_0/\text{K}$
-2.5887	$-4.1302\cdot 10^{-6}$	776.49	2.7918	$-2.6764\cdot 10^{-3}$	188

When fitted to the present experimental data, the parameters given in Table 4 were obtained. The quality of the fit may be quantified by the absolute average relative deviation,

$$\Delta_{\text{AAD}} = \frac{1}{N} \sum_{i=1}^N (|\eta_i - \eta_{i,\text{fit}}|/\eta_i) \quad (6)$$

and the maximum absolute relative deviation,

$$\Delta_{\text{MAD}} = \max(|\eta_i - \eta_{i,\text{fit}}|/\eta_i) \quad (7)$$

where  $\eta_i$  is an experimental datum,  $\eta_{i,\text{fit}}$  is from eq 5 evaluated at the same state point, and  $N$  is the number of points. In the present case,  $\Delta_{\text{AAD}} = 0.9\%$  and  $\Delta_{\text{MAD}} = 2.9\%$ . The relative deviations of the experimental viscosities from the VFT equation

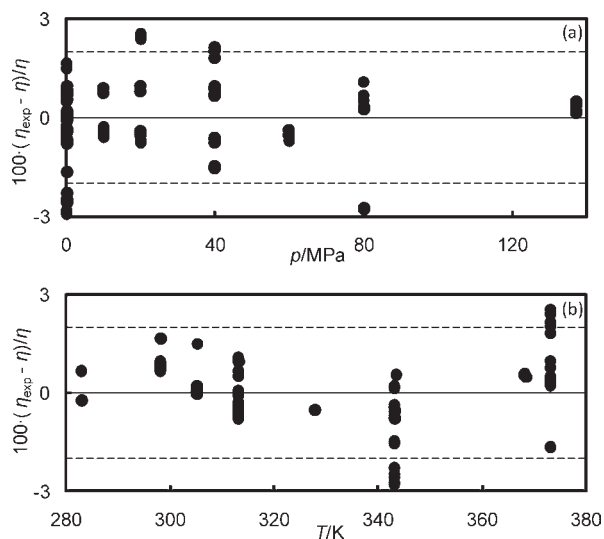


**Figure 5.** Relative deviations of the viscosity of DIDP from eq 5 with parameters from Table 4: (a) as a function of pressure  $p$ ; (b) as a function of temperature  $T$ . Dashed lines indicate the estimated uncertainty of the correlation.

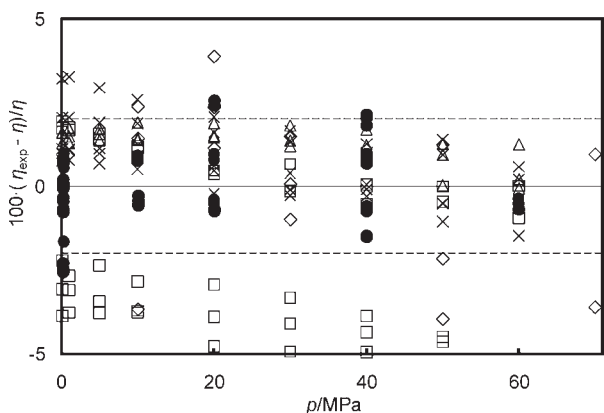


**Figure 6.** Relative deviations of the viscosity of DIDP from eq 5 with parameters from Table 4: ●, this work; □, Paredes et al. (sample A);<sup>13</sup> ×, Paredes et al. (sample B);<sup>13</sup> △, Paredes et al. (sample C);<sup>13</sup> ◇, Motari et al.<sup>14</sup> Dashed lines indicate the estimated uncertainty of the correlation.

are illustrated in Figure 5 as a function of both pressure and temperature. Overall, the VFT provides a satisfactory representation of the experimental results, with 90 % of the data points deviating by less than 2 %.

A number of other workers have reported viscosity measurements on DIDP at elevated pressures. In Figure 6, we compare the present work with that of Paredes et al.,<sup>13</sup> who measured the viscosity of three different samples of DIDP with a rolling ball viscometer at pressures up to 60 MPa and at temperatures between (303.15 and 373.15) K. Their results show quite significant differences between samples but all agree with our measurements and correlation to within  $\pm 5$  %. Their sample “C”, which is from the same lot of DIDP as used in the present work, deviates by only  $\pm 2$  % from our correlation. Also shown in Figure 6 are the results of Al Motari et al.,<sup>14</sup> who measured the viscosity with a vibrating-wire instrument similar to the one used in the present study at temperatures between (298.15 and 373.15) K. Harris and Bair<sup>4</sup> have measured the viscosity of three different samples of DIDP

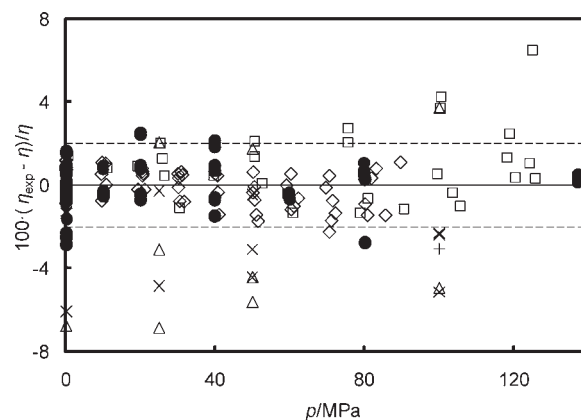


**Figure 7.** Relative deviations of the viscosity of DIDP from eq 5 with parameters from Table 4: ●, this work; □, Harris and Bair (sample B, Canberra viscometer);<sup>4</sup> △, Harris and Bair (sample B, Alpha viscometer);<sup>4</sup> ×, Harris and Bair (sample C, Alpha viscometer);<sup>4</sup> +, Harris and Bair (sample C, MHP viscometer);<sup>4</sup> ◇, Harris.<sup>15</sup> Dashed lines indicate the estimated uncertainty of the correlation.

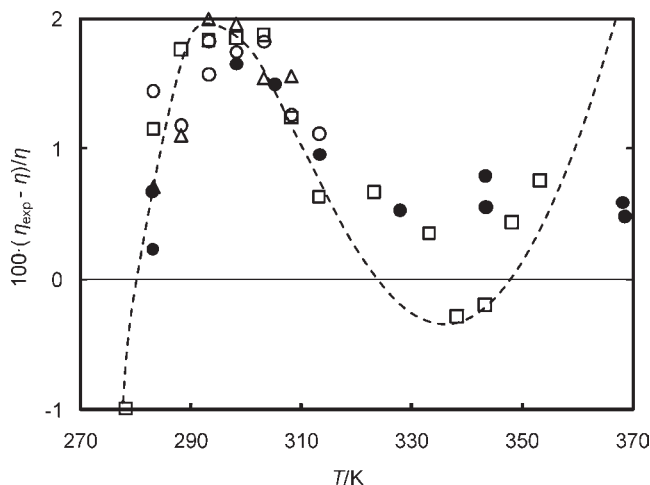


**Figure 8.** Relative deviations of the viscosity of DIDP at  $p = 0.1$  MPa from eq 5 with parameters from Table 4: ●, this work (capillary viscometer); □, Harris and Bair (sample B, Canberra viscometer);<sup>4</sup> ○, Caetano et al.;<sup>18</sup> △, Fröba and Leipertz;<sup>17</sup> ---, eq 8.

with three different falling-body viscometers at pressures up to 1 GPa and at temperatures between (293.15 and 373.15) K. Their results in the overlapping pressure range are compared with the present work in Figure 7. The relative deviations from eq 5 range up to  $\pm 7$  %, but most of the data fall within  $\pm 4$  % of eq 5. The results obtained with the “Canberra” viscometer show the smallest deviations from our correlation with  $\Delta_{\text{AAD}} = 1.6$  %. We also show the recent results of Harris<sup>15</sup> at  $298.15 \leq T/K \leq 348.15$  and pressures up to 90 MPa. These agree remarkably closely with our correlation:  $\Delta_{\text{AAD}} = 0.8$  % and  $\Delta_{\text{MAD}} = 2.3$  %. It is also notable that viscosities as high as 2000 mPa·s are represented in Figure 7 with small deviations from our correlation, despite this being approximately 10 times the greatest viscosity studies in the present work. For example, Harris and Bair<sup>4</sup> report that, at  $T = 293.15$  K and  $p = 118.9$  MPa,  $\eta = 2034$  mPa·s and this value have a relative deviation from our correlation of only 2.5 %. The lowest temperature represented in Figures 6 and 7 is 293.15 K, and hence the applicability of eq 5 at lower temperatures and  $p > 0.1$  MPa is untested.

In Figure 8, we compare our capillary measurements at  $p = 0.1$  MPa with those of other workers who report ambient-pressure viscosities of DIDP. Here we see good agreement between our results and all of the reported data, but a clear systematic deviation which serves to illustrate the limitations of eq 5. An improved representation of the available experimental data at  $p = 0.1$  MPa is provided by the Barlow–Lamb equation,<sup>16</sup>

$$\ln[\eta/(\text{mPa}\cdot\text{s})] = A \exp[B(300 \text{ K}/T)^4] \quad (8)$$

with  $A = 0.7244$  and  $B = 4.687$ . These parameters were obtained by fitting simultaneously our capillary results and the data of Caetano et al.,<sup>2</sup> Harris and Bair (sample B),<sup>4</sup> and Fröba and Leipertz<sup>17</sup> which, together, cover the temperature range (273 to 369) K. For this fit, we find  $\Delta_{\text{AAD}} = 0.5\%$  and  $\Delta_{\text{MAD}} = 1.7\%$ . Equation 8 is in excellent agreement with the reference values reported by Caetano et al.<sup>5</sup> at  $T = (293.15, 298.15, \text{ and } 303.15)$  K, with relative deviation of  $(-0.2, 0.1, \text{ and } 0.2)\%$ , respectively.

## CONCLUSIONS

The present work extends the available data for the viscosity of DIDP. Our results were obtained with an absolute primary viscometer, described by a fully developed working equation, and pertain to a sample of high chemical purity. We present a correlation (eq 5) which is in good agreement with most of the available data and may be recommended for application at pressures up to 140 MPa at temperatures in the range (293.15 to 373.15) K. An alternative correlation (eq 8), based on the present results and data from the literature, is preferred for ambient-pressure applications and is valid for temperatures in the range (273 to 369) K. There appears to be a consensus that, despite ambiguity over the isomeric purity of commercial samples, DIDP might serve as a useful fluid for the calibration of secondary viscometers in an extended range of temperature and pressure.

## AUTHOR INFORMATION

### Corresponding Author

\*E-mail: m.trusler@imperial.ac.uk.

### Funding Sources

This work was supported by Schlumberger Cambridge Research and by the Royal Academy of Engineering.

## ACKNOWLEDGMENT

The authors are grateful to Dr Anthony Goodwin (Schlumberger Technology Corp.) for sourcing the tungsten wire used in this study.

## REFERENCES

- (1) Caetano, F. J. P.; Fareleira, J. M. N. A.; Fernandes, A. C.; Oliveira, C. M. B. P.; Serro, A. P.; de Almeida, I. M. S.; Wakeham, W. A. Diisodecylphthalate (DIDP) - a potential standard of moderate viscosity: Surface tension measurements and water content effect on viscosity. *Fluid Phase Equilib.* **2006**, *245*, 1–5.
- (2) Caetano, F. J. P.; Fareleira, J.; Oliveira, C.; Wakeham, W. A. New measurements of the viscosity of diisodecyl phthalate using a vibrating wire technique. *J. Chem. Eng. Data* **2005**, *50*, 1875–1878.
- (3) Caetano, F. J. P.; Fareleira, J. M. N. A.; Oliveira, C. M. B. P.; Wakeham, W. A. Viscosity of di-isodecylphthalate: A potential standard of moderate viscosity. *Int. J. Thermophys.* **2004**, *25*, 1311–1322.

- (4) Harris, K. R.; Bair, S. Temperature and pressure dependence of the viscosity of diisodecyl phthalate at temperatures between (0 and 100) °C and at pressures to 1 GPa. *J. Chem. Eng. Data* **2007**, *52*, 272–278.

- (5) Caetano, F. J. P.; Fareleira, J. M. N. A.; Froba, A. P.; Harris, K. R.; Leipertz, A.; Oliveira, C. M. B. P.; Trusler, J. P. M.; Wakeham, W. A. An industrial reference fluid for moderately high viscosity. *J. Chem. Eng. Data* **2008**, *53*, 2003–2011.

- (6) Peleties, F. *Advanced Fluid Property Measurement for Oilfield Applications*; Imperial College London: London, 2007.

- (7) Shapal-M Machinable Ceramic Physical Properties. <http://www.precision-ceramics.co.uk/shap3.htm> (accessed Nov 12, 2010).

- (8) Retsina, T.; Richardson, S. M.; Wakeham, W. A. The Theory of a Vibrating-Rod Densimeter. *Appl. Sci. Res.* **1986**, *43*, 127–158.

- (9) Retsina, T.; Richardson, S. M.; Wakeham, W. A. The Theory of a Vibrating-Rod Viscometer. *Appl. Sci. Res.* **1987**, *43*, 325–346.

- (10) Caudwell, D. R.; Trusler, J. P. M.; Vesovic, V.; Wakeham, W. A. Viscosity and Density of Five Hydrocarbon Liquids at Pressures up to 200 MPa and Temperatures up to 473 K. *J. Chem. Eng. Data* **2009**, *54*, 359–366.

- (11) Caudwell, D. R.; Trusler, J. P. M.; Vesovic, V.; Wakeham, W. A. Viscosity and Density of Five Hydrocarbon Liquids at Pressures up to 200 MPa and Temperatures up to 473 K. *J. Chem. Eng. Data* **2010**, *55*, 5396–5396.

- (12) Peleties, F.; Segovia, J. J.; Trusler, J. P. M.; Vega-Maza, D. Thermodynamic properties and equation of state of liquid di-isodecyl phthalate at temperature between (273 and 423) K and at pressures up to 140 MPa. *J. Chem. Thermodyn.* **2010**, *42*, 631–639.

- (13) Paredes, X.; Fandiño, O.; Comuñas, M. J. P.; Pensado, A. S.; Fernández, J. Study of the effects of pressure on the viscosity and density of diisodecyl phthalate. *J. Chem. Thermodyn.* **2009**, *41*, 1007–1015.

- (14) Al Motari, M. M.; Kandil, M. E.; Marsh, K. N.; Goodwin, A. R. H. Density and viscosity of diisodecyl phthalate  $\text{C}_{10}\text{H}_{21}(\text{COOC})_2$ , with nominal viscosity at  $T = 298$  K and  $p = 0.1$  MPa of 87 mPa·s, at temperatures from (298.15 to 423.15) K and pressures up to 70 MPa. *J. Chem. Eng. Data* **2007**, *52*, 1233–1239.

- (15) Harris, K. R. Temperature and Pressure Dependence of the Viscosities of 2-Ethylhexyl Benzoate, Bis(2-ethylhexyl) Phthalate, 2,6,10,15,19,23-Hexamethyltetracosane (Squalane), and Diisodecyl Phthalate. *J. Chem. Eng. Data* **2009**, *54*, 2729–2738.

- (16) Barlow, A. J.; Lamb, J. The visco-elastic behaviour of lubricating oils under cyclic shearing stress. *Proc. R. Soc. London, Ser. A* **1959**, *253*, 52–69.

- (17) Fröba, A. P.; Leipertz, A. Viscosity of diisodecyl phthalate by surface light scattering (SLS). *J. Chem. Eng. Data* **2007**, *52*, 1803–1810.

- (18) Caetano, F. J. P.; Fareleira, J. M. N. A.; Oliveira, C. M. B. P.; Wakeham, W. A. New measurements of the viscosity of diisodecyl phthalate using a vibrating wire technique. *J. Chem. Eng. Data* **2005**, *50*, 1875–1878.